

SHIFTADDAUG: AUGMENT MULTIPLICATION-FREE TINY NEURAL NETWORK WITH HYBRID COMPUTATION

Anonymous authors

Paper under double-blind review

ABSTRACT

1 We introduce a novel training methodology termed **ShiftAddAug** aimed
2 at enhancing the performance of multiplication-free tiny neural networks.
3 Multiplication-free operators, such as Shift and Add, have garnered attention be-
4 cause of their hardware-friendly nature. They are more suitable for deployment
5 on resource-limited platforms with reduced energy consumption and computa-
6 tional demands. However, multiplication-free networks usually suffer from under-
7 performance in terms of accuracy compared to their vanilla counterpart with the
8 same structure. ShiftAddAug uses costly multiplication to augment efficient but
9 less powerful multiplication-free operators, improving network accuracy without
10 any inference overhead. It puts a multiplication-free tiny NN into a large multi-
11 plicative model and encourages it to be trained as a sub-model to obtain additional
12 supervision, rather than as an independent model. In the process of inference, only
13 the multiplication-free tiny model is used. The effectiveness of ShiftAddAug is
14 demonstrated through experiments in image classification, consistently resulting
15 in significant improvements in accuracy and energy saving. **Notably, it achieves up
16 to a 4.95% accuracy improvement on the CIFAR100 compared to multiplication-
17 free counterparts. This result far exceeds the directly trained multiplicative NNs of
18 the same structure.** Additionally, neural architecture search is used to obtain bet-
19 ter augmentation effects and smaller but stronger multiplication-free tiny neural
20 networks. Codes and models will be released upon acceptance.

21 1 INTRODUCTION

22 The application of deep neural networks (DNNs) on resource-constrained platforms is still lim-
23 ited due to their huge energy requirements and computational costs. However, with the increasing
24 popularity of small computing devices such as IoT equipment(Statista, 2016), implementing DNNs
25 directly on these devices can enhance privacy and efficiency. To obtain a small model deployed
26 on edge devices, the commonly used techniques are pruning(Han et al., 2015b; Molchanov et al.,
27 2017), quantization(Han et al., 2015a; Wang et al., 2019), and knowledge distillation(Hinton et al.,
28 2015). There are also some training methods specially designed for tiny neural networks(tiny NNs).
29 NetAug(Cai et al., 2022) believes tiny NNs tend to cause under-fitting results due to limited capacity,
30 so it augments the tiny model by inserting it into a larger models, sharing the weights and gradients.

31 However, the NNs designed by the above works are all based on multiplication, which is not
32 hardware-efficient. The common hardware design practice in computer architecture or digital signal
33 processing tells that multiplication can be replaced by bitwise shifts and additions(Xue & Liu, 1986;
34 Gwee et al., 2009) to achieve faster speed and lower energy consumption. Introducing this idea into
35 NNs design, DeepShift(Elhoushi et al., 2021) and AdderNet(Chen et al., 2020) proposed ShiftConv
36 operator and AddConv operator respectively.

37 This paper takes one step further along the direction of multiplication-free neural networks, propos-
38 ing a method to augment tiny multiplication-free NNs by hybrid computation, which significantly
39 improves accuracy without any inference overhead. Tiny computing devices have more severe com-
40 putational, memory, and energy requirements, which makes using multiplication-free networks a
41 good choice. However, these multiplication-free operators cannot restore all the information from

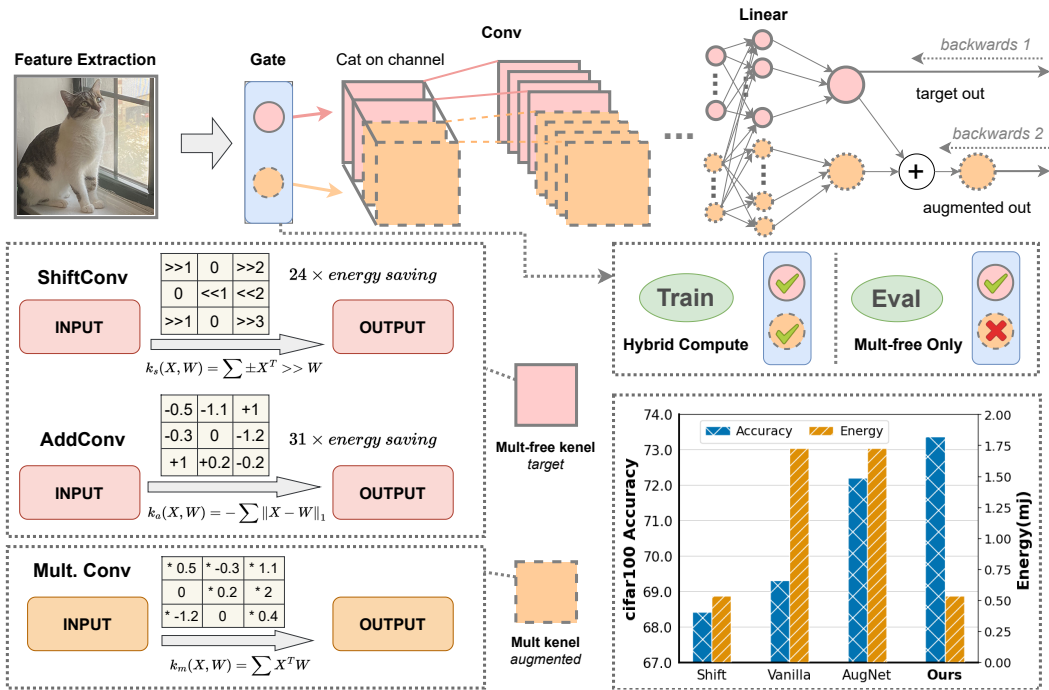


Figure 1: Overview of ShiftAddAug. The solid line and pink modules represent the multiplication-free kernels, which are used to build the target model (Shift or Add); the dotted line and orange modules represent the multiplicative kernels, which are the part that augment the model. We connect this two kinds of operators in the channel dimension for *weight sharing* and *joint training*. In the process of inference, we only retain the multiplication-free part. Obtained models have higher accuracy (up to 4.05%) than their multiplicative counterparts with the same structure, and save 68.9% energy.

42 the original operator, resulting in more serious under-fitting. Instead of converting and fine-tuning
 43 from a well-trained multiplicative model, we choose to build wider hybrid computing NNs, and set
 44 the multiplication-free part as the target model used in inference. We expect the stronger multiplica-
 45 tive part to push the target model to a better condition.

46 We validate our method on MobileNetV2(Sandler et al., 2018), MobileNetV3(Howard et al., 2019),
 47 MCUNet(Lin et al., 2020), ProxylessNAS(Cai et al., 2019), MobileNetV2-Tiny(Lin et al., 2020).
 48 Compared with the multiplicative networks of the same structure, we have significant accuracy im-
 49 provements (1.24%~4.05%) on the CIFAR100 dataset and obtain considerable speed improvement
 50 ($2.94 \times$ to $3.09 \times$) and energy saving (67.75%~69.09%). To further improve the performance, we
 51 introduce neural architecture search(NAS) into our work, proposing a new method for searching
 52 more efficient multiplication-free tiny neural networks. Our contributions can be summarized as
 53 follows:

- 54 • For the multiplication-free tiny neural network, we propose a hybrid computing augmenta-
 55 tion method using multiplicative operators to augment the target multiplication-free network.
 56 Under the same model structure, it is more expressive and ultra-efficient.
- 57 • We propose a new weight sharing strategy for hybrid computing augmentation, which solves
 58 the weight tearing problem in heterogeneous (e.g., Gaussian vs. Laplacian) weight sharing
 59 during the augmentation process.
- 60 • We design a hardware-aware neural architecture search strategy based on hybrid computing
 61 augmentation. We start training with an costly model and let some parts of it fade away to
 62 meet the hardware constraints in the training process. NAS will search for shrinking solutions
 63 to further boost accuracy.

64 2 RELATED WORKS

65 **Multiplication-Free NNs.** In order to reduce the intensive multiplication that occupies the main
 66 energy and time consumption, an important trend is to use hardware-friendly operators instead of
 67 multiplications. ShiftNet(Wu et al., 2018; Chen et al., 2019) believes that the Shift can be regarded
 68 as a special case of Depthwise Convolution, and proposes a zero-parameter, zero-flop convolution
 69 operator. DeepShift(Elhoushi et al., 2021) retains the calculation method of original convolution,
 70 but replaces the multiplication with bit-shift and bit-reversal. BNNs(Courbariaux et al., 2016; Lin
 71 et al., 2016; Rastegari et al., 2016) binarize the weight or activation to build DNNs consisting of sign
 72 changes, and get faster calculation in hardware by *xnor*. AdderNet (Chen et al., 2020; Song et al.,
 73 2021) chooses to replace multiplicative convolution with less expensive addition, and design an
 74 efficient hardware implementation(Wang et al., 2021). ShiftAddNet(You et al., 2020) combines bit-
 75 shift and add. It gets up to $196\times$ energy savings on hardware as shown in Tab. 1. ShiftAddVit(You
 76 et al., 2023) puts this idea into vision transformer and performs hybrid computing through mixture
 77 of experts.

78 **Network Augmentation.** The tiny neural network is developing
 79 rapidly. Networks and optimization techniques designed for MCU
 80 have already appeared at present(Lin et al., 2020; 2021a). It is
 81 also possible to train under the 256KB memory limit(Lin et al.,
 82 2022). Due to the smaller capacity, the training of tiny NNs will
 83 have more challenges. Once-for-all(Cai et al., 2020) proposes the
 84 Progressive Shrinking training method, and finds that the accu-
 85 racy of the obtained model is better than the same network that
 86 trained from scratch. Inspired by this result, NetAug(Cai et al.,
 87 2022) raises a point that tiny neural networks need more capaci-
 88 ty rather than noise in training. Therefore, they chose a scheme
 89 that is the opposite of network structure regularization methods
 90 like Dropout(Srivastava et al., 2014), StochasticDepth(Huang et al.,
 91 2016), DropBlock(Ghiasi et al., 2018): expand the model width and
 92 let the large model lead the small model to achieve better accuracy
 93 through weight sharing.

94 **Neural Architecture Search.** NAS has achieved amazing success in automating the design of ef-
 95 ficient NN architectures(Liu et al., 2019b;a). In addition to obtain higher accuracy, some works
 96 include hardware performance of the model, such as latency(Tan et al., 2019; Wu et al., 2019) and
 97 memory(Lin et al., 2020), into the search. In parts that are closer to the hardware, NAS can also
 98 be used to explore faster operator implementations(Chen et al., 2018) and combine network struc-
 99 tures for optimization(Lin et al., 2021b; Shi et al., 2022). BossNAS(Li et al., 2021) searched the
 100 network of hybrid CNN-transformers structure and ShiftAddNAS(You et al., 2022) for the first time
 101 constructed a search space with mixed multiplication and multiplication-free operators. However,
 102 unlike our target, networks the ShiftAddNAS focuses on are far beyond the hardware limitations of
 103 edge devices.

104 3 SHIFTADDAUG

105 In this section, we introduce the hybrid computing augmentation method and then present our het-
 106 erogeneous weight sharing strategy to solve the weight-tearing problem. In the end, we introduce a
 107 new hardware-aware NAS method to get better multiplication-free tiny NNs.

108 3.1 PRELIMINARIES

109 **Shift.** For the shift operator, training is similar to the regular approach of linear or convolution
 110 operators with weight W , but round it to the nearest power of 2. During inference, use bit-shift and
 111 bit-reversal to efficiently get the same calculation result as Equ. 1. All inputs are quantized before
 112 calculation and dequantized when the output is obtained.

Table 1: Hardware cost under 45nm CMOS.

OPs	Format	Energy (pJ)
Mult.	FP32	3.7
	FP16	0.9
	INT32	3.1
	INT8	0.2
Add	FP32	1.1
	FP16	0.4
	INT32	0.1
	INT8	0.03
Shift	INT32	0.13
	INT16	0.057
	INT8	0.024

$$\begin{cases} \mathbf{S} = \text{sign}(\mathbf{W}) \\ \mathbf{P} = \text{round}(\log_2(|\mathbf{W}|)) \end{cases} \rightarrow \begin{cases} \mathbf{Y} = \mathbf{X}\tilde{\mathbf{W}}_g^T = \mathbf{X}(\mathbf{S} \cdot 2^{\mathbf{P}})^T, & \text{train.} \\ \mathbf{Y} = \sum_{i,j} \sum_k \pm(X_{i,k} \gg P_{k,j}), & \text{infer.} \end{cases} \quad (1)$$

113 **Add.** Add operator replaces multiplication in original convolutions with subtractions and ℓ_1 dis-
114 tance, since subtractions can be easily reduced to additions by using complement code.

$$Y_{m,n,t} = - \sum_{i=0}^d \sum_{j=0}^d \sum_{k=0}^{c_{in}} |X_{m+i,n+j,k} - F_{i,j,k,t}|. \quad (2)$$

115 **NetAug.** Network Augmentation encourages the tiny NNs to work as a sub-model of a large model
116 expanded in width. Based on shared weights, the target tiny NN and the augmented large model are
117 jointly trained. The training loss and parameter updates are as follows:

$$\mathcal{L}_{aug} = \mathcal{L}(\mathbf{W}_t) + \alpha \mathcal{L}(\mathbf{W}_a), \quad \mathbf{W}_t^{n+1} = \mathbf{W}_t^n - \eta \left(\frac{\partial \mathcal{L}(\mathbf{W}_t^n)}{\partial \mathbf{W}_t^n} + \alpha \frac{\partial \mathcal{L}(\mathbf{W}_a^n)}{\partial \mathbf{W}_t^n} \right). \quad (3)$$

118 where \mathcal{L} is the loss function, \mathbf{W}_t is the weight of the target tiny NN, \mathbf{W}_a is the weight of the
119 augmented NN, and \mathbf{W}_t is a subset of \mathbf{W}_a .

120 3.2 HYBRID COMPUTING AUGMENT

121 Our method is designed for tiny multiplication-free CNNs, introducing multiplication in the training
122 process, and using only multiplication-free operators during inference as possible to improve the
123 speed and save more energy. We combine the convolution kernels of different operators on the
124 channel dimension as shown in Fig. 1. The target model will use multiplication-free convolution
125 (MFConv, ShiftConv(Elhoushi et al., 2021) or AddConv(Chen et al., 2020) can be chosen), then
126 take multiplicative convolution (MConv, i.e. original Conv) as the augmented part.

127 Since NetAug widens the channel and increases the expanding ratio of the Inverted Block, the input
128 of each convolution in the large model can be conceptually split into the target part \mathbf{X}_t and the
129 augmented part \mathbf{X}_a , so does the output $\mathbf{Y}_t, \mathbf{Y}_a$. In our work, \mathbf{X}_t and \mathbf{Y}_t mainly carry information of
130 MFConv, while \mathbf{X}_A and \mathbf{Y}_A are obtained by original Conv.

131 Here we mainly discuss three types of operators commonly used to build augmented tiny NNs:
132 Convolution (Conv), Depthwise Convolution (DWConv), and Fully Connected (FC) layer. The
133 hybrid computing augmentation for DWConv is the most intuitive. We only need to split the input
134 into \mathbf{X}_t and \mathbf{X}_a , then use MFConv and MConv to calculate respectively and connect the obtained
135 \mathbf{Y}_t and \mathbf{Y}_a in the channel dimension. For Conv, We use all input \mathbf{X} to get \mathbf{Y}_a through MConv. But
136 to get \mathbf{Y}_t , we still need to split the input and calculate it separately, and finally add the results. Since
137 the FC layer is only used as a classification head, its output does not require augmentation. We
138 divide the input and use Linear and ShiftLinear to calculate respectively, and add the results. If bias
139 is used, it will be preferentially bounded to multiplication-free operators.

$$\begin{aligned} DWConv : & \begin{cases} \mathbf{Y}_t = \text{MFConv}(\mathbf{X}_t) \\ \mathbf{Y}_a = \text{MConv}(\mathbf{X}_a) \\ \mathbf{Y} = \text{cat}(\mathbf{Y}_t, \mathbf{Y}_a) \end{cases}, & FC : & \begin{cases} \mathbf{Y}_t = \text{ShiftLinear}(\mathbf{X}_t) \\ \mathbf{Y}_a = \text{Linear}(\mathbf{X}) \\ \mathbf{Y} = \mathbf{Y}_t + \mathbf{Y}_a \end{cases}, \\ Conv : & \begin{cases} \mathbf{Y}_t = \text{MFConv}(\mathbf{X}_t) + \text{MConv}(\mathbf{X}_a) \\ \mathbf{Y}_a = \text{MConv}(\mathbf{X}) \\ \mathbf{Y} = \text{cat}(\mathbf{Y}_t, \mathbf{Y}_a) \end{cases} \end{aligned} \quad (4)$$

140 3.3 HETEROGENEOUS WEIGHT SHARING

141 **Dilemma.** Weight sharing strategy is widely used in one-shot neural architecture search(Guo et al.,
142 2020; Yu et al., 2020) and multi-task learning(Ruder, 2017). In Network Augmentation, to learn the
143 most important information in the large network, the ℓ_1 norm is calculated for the weight of each

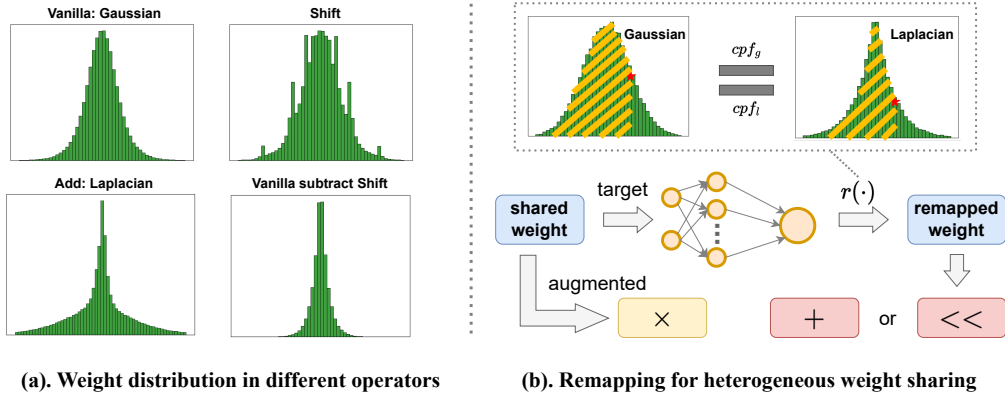


Figure 2: *Left*: Weight distribution of different convolution operators for MobileNetV2. Inconsistent weight distribution leads to tearing problems, making weight sharing difficult. *Right*: Through our weight remapping strategy, different operators can share a weight pool. For ShiftConv, the mapping result is only used as a bias.

144 channel at the end of every epoch. The important weights will be redirected to the target model.
 145 This looks like Channel-level Pruning(Mao et al., 2017), but different in the training process.

146 However, since the weight distribution of the multiplication-free operator is inconsistent with original Conv, it causes the weight tearing problem. As shown in Fig. 2(a), the weight in original Conv conform to Gaussian distribution, while ShiftConv has spikes at some special values. We find that the weight in ShiftConv is the one of original Conv plus a Laplace distribution with a small variance. The weight in AddConv conforms to the Laplace distribution. ShiftAddNas(You et al., 2022) adds a penalty term to the loss function, and guides the weight in heterogeneous operators to conform to the same distribution. Although this can alleviate the problem, it affects the network to achieve its maximum performance, which is more serious on tiny NNs with smaller capacity.

154 **Solution: heterogeneous weight sharing.** To solve the above dilemma, we propose a new heterogeneous weight sharing strategy for the shift and add operators. This method is based on original Conv and passes parameters to weights of different distribution types through a mapping function $\mathcal{R}(\cdot)$. Considering that the weights of original Conv and ShiftConv still have a deep relation, we hope to get a suitable bias to compensate for the weight when mapping to ShiftConv. For AddConv, we directly use the same method to get a new weight for replacement.

160 When mapping the Gaussian distribution to the Laplace distribution, we hope that the cumulative probability of the original value and mapping result are the same. Firstly, calculate the cumulative probability of the original weight in Gaussian. Then put the result in the percent point function of Laplacian. The workflow is shown in Fig. 2(b). The mean and standard deviation of the Gaussian can be calculated through the weights, but for the Laplace, these two values need to be determined through prior knowledge.

$$\begin{aligned}
 \mathbf{W}_l &= \mathcal{R}(\mathbf{W}_g) = r(\text{FC}(\mathbf{W}_g)), & \text{cpf}_g(x) &= \frac{1}{\sigma\sqrt{2\pi}} \int_{-\infty}^x e^{-\frac{(x-\mu)^2}{2\sigma^2}} dx, \\
 r(\cdot) &= \text{ppf}_l(\text{cpf}_g(\cdot)), & \text{ppf}_l(x) &= \mu - b * \text{sign}(x - \frac{1}{2}) * \ln(1 - 2|x - \frac{1}{2}|).
 \end{aligned}
 \tag{5}$$

166 Where \mathbf{W}_g is the weight in original Conv that conforms to the Gaussian distribution, and \mathbf{W}_l is the weight obtained by mapping that conforms to the Laplace distribution. FC is a fully connected layer. We need this because the weights don't fit the Distribution perfectly. $\text{cpf}_g(\cdot)$ is the cumulative probability function of Gaussian, $\text{ppf}_l(\cdot)$ is the percentage point function of Laplace.

170 3.4 NERUAL ARCHTECTURE SEARCH

171 We take our proposed method one step further and use neural architecture search to design more
 172 efficient yet powerful multiplication-free models. Our method mainly aims to enhance the effect of
 173 hybrid computing augmentation.

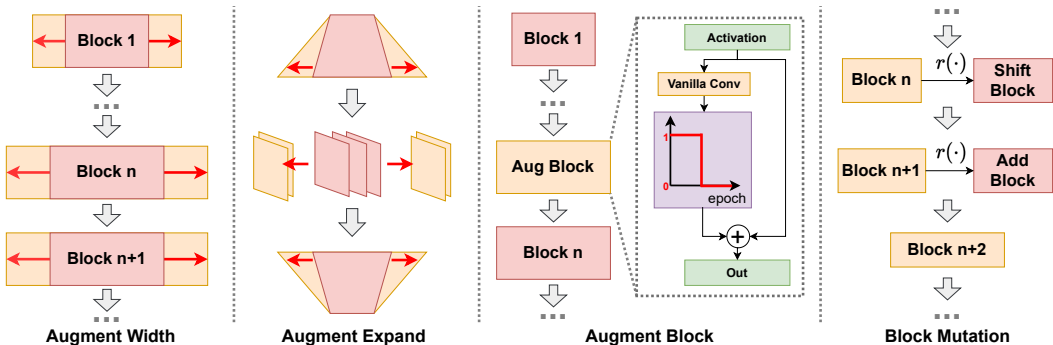


Figure 3: Methods used to construct search spaces. *Augment Width*: use MConv to widen the MFConv channel; *Augment Expand*: increase expand ratio of InvertedBlock, i.e. the channels of depthwise separable convolution; *Augment Block*: select some blocks and make them fade away during training for target model; *Block Mutation*: based on MConv, mutate the block into ShiftConv or AddConv.

174 We follow tinyNAS(Lin et al., 2020) to build our
 175 search space of model structure and set energy and
 176 latency limit of the target model to help us priori-
 177 tize the elimination of some expensive model struc-
 178 tures. Let the set of model structures that satisfy the
 179 hardware constraints be \mathbb{T} , and the set of all feasible
 180 model structures be \mathbb{A} . We first select the structure
 181 and operator type of the target model, and verify whether it belongs to the \mathbb{T} . If so, we create its
 182 counterpart, which is in the \mathbb{A} but not in the \mathbb{T} , and transition it into the \mathbb{T} during training. To achieve
 183 this, we use Augment Block and Block Mutation.

184 **Augment Block** is intended to insert some multiplication blocks into the backbone to help the target
 185 model extract more information during early training. It will then fade away in the target model but
 186 remain in the augmented one. In other words, this is an augmentation at the depth of the model. As
 187 for **Block Mutation**, although the operator type of the target model is determined at the beginning
 188 of each search, it lets the model use more powerful multiplicative operators in the early stage, and
 189 mutate to more efficient Shift or Add operators during the training process.

190 Combining the Width Augmentation and Expand Augmentation we used in section 3.2, we construct
 191 our search space according to Tab. 2. The schematic diagram of the four augmentation methods is
 192 shown in Fig. 3. We then perform an evolution search to find the best model within the search space.

Table 2: Search space of ShiftAddAug.

Block types	[Conv, Shift, Add]
width aug. multiples	[2.2, 2.4, 2.8, 3.2]
expand aug. multiples	[2.2, 2.4, 2.8, 3.2]
block aug. index	[None, 1, 2, 3]

193 4 EXPERIMENTS

194 4.1 SETUP

195 **Datasets.** We conduct experiments on several image classification datasets, including
 196 ImageNet-1K(Deng et al., 2009), CIFAR10(Krizhevsky, 2009), CIFAR100(Krizhevsky, 2009),
 197 Food101(Bossard et al., 2014), Flowers102 (Nilsback & Zisserman, 2008), Cars(Krause et al.,
 198 2013), Pets(Parkhi et al., 2012) and OpenEDS(Palmero et al., 2020) for segmentation task.

199 **Training Details.** We follow the training process in NetAug(Cai et al., 2022) and train models with
 200 batch size 128 using 2 GPUs. We use the SGD optimizer with Nesterov momentum 0.9 and weight
 201 decay $4e-5$. By default, the Baseline and Shift models are trained for 250 epochs, and Add models
 202 are trained for 300 epochs. The initial learning rate is 0.05 and gradually decreases to 0 following
 203 the cosine schedule. Label smoothing is used with a factor of 0.1. Please refer to Appendix E for
 204 more details.

205 **Hardware Performance.** Since many works have verified the efficiency of shift and add on pro-
 206 prietary hardware(You et al., 2020; 2022; Wang et al., 2021; You et al., 2023), we follow their
 207 evaluation metrics. Hardware energy and latency are measured based on a simulator of Eyeriss-like

Table 3: ShiftAddAug vs. Multiplicative Baseline in terms of accuracy and efficiency on CIFAR100 classification tasks. ShiftAddAug not only improves the accuracy of popular tiny neural networks but also achieves better speed and energy efficiency. Please refer to Appendix.B for the specific meaning of each method.

Model	Method	Params (M)	Mult (M)	Shift (M)	Add (M)	Accuracy(%)	Energy (mj)	Latency (ms)
MobileNetV2 w0.35	Base / NetAug	0.52	29.72	0	29.72	70.59 / 71.98	2.345	0.73
	Shift / AugShift	0.52	0	29.72	29.72	69.25 / 71.83 ($\uparrow 2.58$)	0.74	0.246
	Add / AugAdd	0.52	4.52	0	56.88	67.85 / 69.38 ($\uparrow 1.5$)	1.091	0.753
MobileNetV3 w0.35	Base / NetAug	0.96	18.35	0	18.35	69.32 / 72.2	1.726	0.485
	Shift / AugShift	0.96	0	18.35	18.35	68.42 / 73.37 ($\uparrow 4.95$)	0.536	0.16
	Add / AugAdd	0.96	3.5	0	34.34	- / -	0.699	0.512
MCUNet	Base / NetAug	0.59	65.72	0	65.72	71.38 / 73.15	4.28	1.682
	Shift / AugShift	0.59	0	65.72	65.72	70.87 / 74.59 ($\uparrow 3.72$)	1.323	0.545
	Add / AugAdd	0.59	20.91	0	113.09	70.25 / 72.72 ($\uparrow 2.47$)	2.345	1.72
ProxylessNAS w0.35	Base / NetAug	0.63	34.56	0	34.56	70.86 / 72.32	2.471	0.883
	Shift / AugShift	0.63	0	34.56	34.56	70.54 / 73.86 ($\uparrow 3.32$)	0.774	0.294
	Add / AugAdd	0.63	8.81	0	61.97	68.87 / 70.18 ($\uparrow 1.31$)	1.281	0.881
MobileNetV2 -Tiny	Base / NetAug	0.35	27.31	0	27.31	69.3 / 71.62	2.161	0.67
	Shift / AugShift	0.35	0	27.31	27.31	68.29 / 71.89 ($\uparrow 3.6$)	0.697	0.228
	Add / AugAdd	0.35	4.43	0	52.09	66.57 / 67.65 ($\uparrow 1.08$)	0.999	0.693

Table 4: Accuracy of MobileNetV2 (w0.35) and MCUNet on more datasets. Training with ShiftAddAug can improve model performance without any overhead during inference on fine-grained classification tasks.

Model	Methods	CIFAR10	ImageNet	Food101	Flower102	Cars	Pets
MobileNetV2 - w0.35	Shift	88.59	51.92	72.99	92.25	72.83	75.4
	AugShift	92.51	53.86	74.67	96.08	74.47	79.59
MCUNet	Shift	90.61	56.45	78.46	95.59	80.51	79.67
	AugShift	93.08	57.34	79.96	97.06	83.29	83.95

208 hardware accelerator(Chen et al., 2017; Zhao et al., 2020), which calculates not only computational
209 but also data movement energy.

210 4.2 SHIFTADDAUG VS. BASELINE

211 We validate our method on MobileNetV2, MobileNetV3, MCUNet, ProxylessNAS and
212 MobileNetV2-Tiny. ShiftAddAug provides consistent accuracy improvements (average $\uparrow 2.82\%$) for
213 ShiftConv augmentation over the multiplicative baselines. For AddConv augmentation, it improves
214 the accuracy compared with direct training (average $\uparrow 1.59\%$). The resulting model will be faster
215 ($3.0\times$ for Shift) and more energy-efficient ($\downarrow 68.58\%$ for Shift and $\downarrow 52.02\%$ for Add) due to the use
216 of hardware-friendly operators. As shown in Tab. 3, these multiplication-free operators usually hurt
217 the performance of the network. Changing all operators to Shift will cause $\downarrow 0.82\%$ accuracy drop on
218 average compared to the multiplication baseline. But after using our method, the accuracy increased
219 by $\uparrow 3.63\%$ on average under the same energy cost.¹

220 In addition, our method achieves higher results than multiplicative NetAug on some models (Mo-
221 bileNetV3: $\uparrow 1.17\%$, MCUNet: $\uparrow 1.44\%$, ProxylessNAS: $\uparrow 1.54\%$). This means that our method enables
222 the multiplication-free operator to be stronger than those of the original operator.

223 To verify the generality of our method, we also conduct experiments on more datasets. As shown
224 in Tab. 4, our method can achieve $\uparrow 0.89\%$ to $\uparrow 4.28\%$ accuracy improvements on different datasets.
225 Hybrid computing augmentation works better on smaller models and datasets with less classification.
226 On Flower102, MobileNetV2-w0.35 has $\uparrow 3.83\%$ accuracy improvements with our method, while
227 MCUNet has only $\uparrow 1.47\%$. This shows that smaller model capacity can achieve better effect on this
228 dataset. The larger the model, the smaller the gain brought by augmentation. The same phenomenon
229 also occurs in CIFAR10. But for bigger datasets such as ImageNet, even if it is augmented, the

¹Loss diverges when we use AddConv on MobileNetV3, both direct training and augmented training.

Table 5: ShiftAddAug vs. SOTA NAS method for hybrid operators in terms of accuracy and efficiency on CIFAR-10/100 classification tasks. ShiftAddAug can further improve the performance of the obtained multiplication-free model.

Model	Method	Resolution	Mult (M)	Shift (M)	Add (M)	Accuracy(%)	MACs Saving
CIFAR10	ShiftAddNas (Mult-free)	32	2	26	38	91.32	-
	ShiftAddNas	32	17	19	58	95.83	-
	ShiftAddAug (Mult-free)	160	0.13	27	27.1	93.43(↑2.11)	17.9%
	ShiftAddAug	96	12.3	14.5	28	95.92(↑0.09)	40.4%
CIFAR100	ShiftAddNas (Mult-free)	32	3	35	48	71.0	-
	ShiftAddNas	32	22	21	62	78.6	-
	ShiftAddAug (Mult-free)	160	0.13	33.5	33.6	74.61(↑3.61)	21.9%
	ShiftAddAug	160	21	17	51	76.21	15.2%
	ShiftAddAug	96	16.2	20.2	36.4	78.72(↑0.12)	33.8%

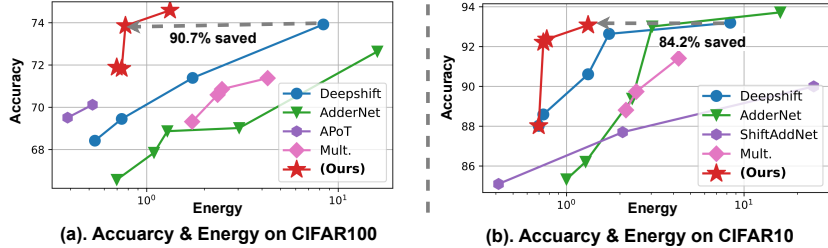


Figure 4: Accuracy and energy cost of ShiftAddAug over SOTA manually designed multiplication-free model and tiny multiplicative models. Tested on CIFAR-100/10.

230 capacity of the model is still not enough. It only achieves $\uparrow 1.94\%$ for MobileNetV2-w0.35 and
 231 $\uparrow 0.89\%$ for MCUNet on ImageNet. For segmentation task, please refer to Appendix. D.

232 4.3 SHIFTADDAUG VS. SOTA MULT.-FREE MODELS

233 We further compare ShiftAddAug over SOTA multiplication-free models, which are designed man-
 234 nually for tiny computing devices, on CIFAR-10/100 to evaluate its effectiveness. As shown in Fig.
 235 4, the base models we use are smaller and have better energy performance. With ShiftAddAug, the
 236 accuracy still exceeds existing work. For DeepShift and AdderNet, our method boosts $\uparrow 0.67\%$ and
 237 $\uparrow 1.95\%$ accuracy on CIFAR100 with $\downarrow 84.17\%$ and $\downarrow 91.7\%$ energy saving. Compared with the SOTA
 238 shift quantization method APoT(Li et al., 2020), we achieve an improved accuracy of $\uparrow 3.8\%$. With
 239 the same accuracy on CIFAR10, our model saves $\downarrow 84.2\%$ of the energy compared with Deepshift,
 240 and $\downarrow 56.45\%$ of the energy compared with AdderNet.

241 4.4 SHIFTADDAUG WITH NEURAL ARCHITECTURE SEARCH

242 Based on hybrid computing augmentation, we introduce neural architecture search into our method
 243 to get stronger tiny neural networks. We conduct our experiments on CIFAR-10/100 and compare
 244 them with the results of ShiftAddNas(You et al., 2022) under similar calculation amounts. As
 245 shown in Tab. 5, the multiplication-free model we obtained achieved higher accuracy ($\uparrow 2.11\%$ and
 246 $\uparrow 3.61\%$) than ShiftAddNas with FBNet(Wu et al., 2019) search space. For hybrid-computed models,
 247 we have to use a smaller input resolution (96 instead of 160) and larger models. While the input
 248 resolution of ShiftAddNas is 32, this gives us $9\times$ the number of calculations at the same model size.
 249 Even so, we can still save 37.1% of calculations on average with similar accuracy.

250 4.5 ABLATION STUDY

251 **Hybrid Computing Augment.** In order to prove that hybrid computing works better, we add an
 252 experiment using only multiplication-free operators for augmentation. We exert experiments based
 253 on NetAug, and replace all the original operators with Shift operators. The difference from our
 254 method is that the Shift operator is also used in the augmentation part, while our method uses the
 255 multiplicative operator in it. As shown in Tab. 6, it yields an average accuracy improvement of
 256 $\uparrow 1.40\%$.

Table 6: The ablation study of hybrid computing augmentation and heterogeneous weight sharing in terms of accuracy on CIFAR100.

Method	MobileNetV2	MobileNetV3	MCUNet	ProxylessNAS	MobileNetV2
	w0.35	w0.35		w0.35	Tiny
Mult. baseline	70.59	69.32	71.38	70.86	69.3
To shift op	69.25	68.42	70.87	70.54	68.29
Aug. with Shift	70.12	71.56	72.68	70.91	69.28
Aug. with Hybrid Computation	69.41	69.63	71.02	70.6	68.45
Aug. with HWS	71.83	73.37	74.59	73.86	71.89

Table 7: The ablation study of block augmentation and block mutation in terms of accuracy on CIFAR100. Results are obtained by neural architecture search.

Method	Mult (M)	Shift (M)	Add (M)	Accuracy(%)	Energy (mj)	Latency (ms)
Aug. Width & Expand	3.7	61	65	75.13	1.52	0.57
Aug. Width & Expand & Block	1.5	56	64.3	75.63	1.42	0.66
Aug. Width & Expand, Mutation	0.6	58	67	75.92	1.4	0.67
All	0.1	71.9	72	76.35	1.632	0.554

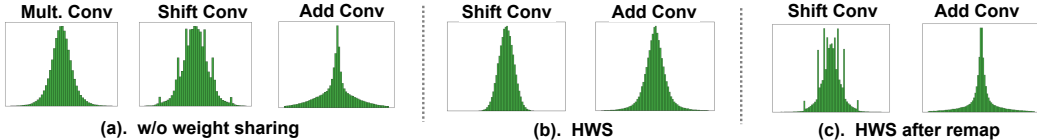


Figure 5: The weight distribution of original Conv / ShiftConv / AddConv layers

257 Then without using the heterogeneous weight sharing (HWS) method, only augmenting tiny NNs
 258 with multiplicative operator will cause $\downarrow 1.09\%$ accuracy drop on average due to the weight tearing
 259 problem. However, the situation changed after we applied for HWS. Compared with using the shift
 260 operator for augmentation, the accuracy increased by $\uparrow 2.2\%$.

261 **Heterogeneous Weight Sharing.** Since the help of HWS on training results has been discussed
 262 above, here we visualize the weight distributions of Conv layers in tiny NNs under three scenarios,
 263 (a) w/o weight sharing; (b) heterogeneous weight sharing; (c) weight after remapped, as shown
 264 in Fig. 5. We consistently observe that the three operators exhibit different weight distributions
 265 without weight sharing. With our HWS, the saved weights are based on the original Conv and
 266 conform to Gaussian distribution. After remapping, the weights can show different distribution
 267 states in Shift/Add Conv calculations. Please refer to Appendix.C for more ablation study of HWS.

268 **Neural Architecture Search.** Our neural architecture search approach is dependent on our pro-
 269 posed hybrid computing augmentation. And it can help the multiplication-free operator to be as
 270 strong as the original operator. Block augmentation and block mutation help us further improve the
 271 performance of multiplication-free tiny NNs. As shown in Tab. 7, under similar energy consump-
 272 tion and latency, block augmentation improves accuracy by $\uparrow 0.5\%$, and block mutation improves by
 273 $\uparrow 0.79\%$. Combining all method, the accuracy of the target model is increased by $\uparrow 1.22\%$.

274 5 CONCLUSION

275 In this paper, we propose ShiftAddAug for training multiplication-free tiny neural networks, which
 276 can greatly improve model accuracy without expanding the model size. It exceeds the multiplia-
 277 tive model in terms of accuracy under the same structure. It's achieved by putting the target
 278 multiplication-free tiny NN into a larger multiplicative NN to get auxiliary supervision. To re-
 279 locate important weights into the target model, we also propose a novel heterogeneous weight sharing
 280 strategy to approach the tearing problem caused by inconsistent weight distribution. Based on
 281 the work above, we use neural architecture search to design more powerful models. Extensive exper-
 282 iments on image classification task consistently demonstrate the effectiveness of ShiftAddAug on
 283 the training process of multiplication-free tiny neural networks.

284 REFERENCES

- 285 Lukas Bossard, Matthieu Guillaumin, and Luc Van Gool. Food-101 – mining discriminative com-
 286 ponents with random forests. In David Fleet, Tomas Pajdla, Bernt Schiele, and Tinne Tuytelaars
 287 (eds.), European Conference on Computer Vision, pp. 446–461, Cham, 2014. Springer Interna-
 288 tional Publishing.
- 289 Han Cai, Ligeng Zhu, and Song Han. Proxylessnas: Direct neural architecture search on target task
 290 and hardware. In International Conference on Learning Representations, 2019.
- 291 Han Cai, Chuang Gan, Tianzhe Wang, Zhekai Zhang, and Song Han. Once-for-all: Train one
 292 network and specialize it for efficient deployment. In International Conference on Learning
 293 Representations, 2020.
- 294 Han Cai, Chuang Gan, Ji Lin, and song han. Network augmentation for tiny deep learning. In
 295 International Conference on Learning Representations, 2022.
- 296 Hanting Chen, Yunhe Wang, Chunjing Xu, Boxin Shi, Chao Xu, Qi Tian, and Chang Xu. Addernet:
 297 Do we really need multiplications in deep learning? In 2020 IEEE/CVF Conference on Computer
 298 Vision and Pattern Recognition (CVPR), pp. 1465–1474, 2020. doi: 10.1109/CVPR42600.2020.
 299 00154.
- 300 Tianqi Chen, Thierry Moreau, Ziheng Jiang, Lianmin Zheng, Eddie Yan, Meghan Cowan, Haichen
 301 Shen, Leyuan Wang, Yuwei Hu, Luis Ceze, Carlos Guestrin, and Arvind Krishnamurthy. Tvm:
 302 An automated end-to-end optimizing compiler for deep learning, 2018.
- 303 Weijie Chen, Di Xie, Yuan Zhang, and Shiliang Pu. All you need is a few shifts: Designing ef-
 304 ficient convolutional neural networks for image classification. In Proceedings of the IEEE/CVF
 305 Conference on Computer Vision and Pattern Recognition (CVPR), June 2019.
- 306 Yu-Hsin Chen, Tushar Krishna, Joel S. Emer, and Vivienne Sze. Eyeriss: An energy-efficient re-
 307 configurable accelerator for deep convolutional neural networks. IEEE Journal of Solid-State
 308 Circuits, 52(1):127–138, 2017. doi: 10.1109/JSSC.2016.2616357.
- 309 Matthieu Courbariaux, Itay Hubara, Daniel Soudry, Ran El-Yaniv, and Yoshua Bengio. Binarized
 310 neural networks: Training deep neural networks with weights and activations constrained to +1
 311 or -1, 2016.
- 312 Jia Deng, Wei Dong, Richard Socher, Li-Jia Li, Kai Li, and Li Fei-Fei. Imagenet: A large-scale hier-
 313 archical image database. In 2009 IEEE Conference on Computer Vision and Pattern Recognition,
 314 pp. 248–255, 2009. doi: 10.1109/CVPR.2009.5206848.
- 315 Mostafa Elhoushi, Zihao Chen, Farhan Shafiq, Ye Henry Tian, and Joey Yiwei Li. Deepshift:
 316 Towards multiplication-less neural networks. In Proceedings of the IEEE/CVF Conference on
 317 Computer Vision and Pattern Recognition (CVPR) Workshops, pp. 2359–2368, June 2021.
- 318 Golnaz Ghiasi, Tsung-Yi Lin, and Quoc V Le. Dropblock: A regularization method for convolu-
 319 tional networks. In S. Bengio, H. Wallach, H. Larochelle, K. Grauman, N. Cesa-Bianchi, and
 320 R. Garnett (eds.), Advances in Neural Information Processing Systems, volume 31. Curran Asso-
 321 ciates, Inc., 2018.
- 322 Zichao Guo, Xiangyu Zhang, Haoyuan Mu, Wen Heng, Zechun Liu, Yichen Wei, and Jian Sun.
 323 Single path one-shot neural architecture search with uniform sampling. In European Conference
 324 on Computer Vision, 2020.
- 325 Bah-Hwee Gwee, Joseph S. Chang, Yiqiong Shi, Chien-Chung Chua, and Kwen-Siong Chong. A
 326 low-voltage micropower asynchronous multiplier with shift–add multiplication approach. IEEE
 327 Transactions on Circuits and Systems I: Regular Papers, 56(7):1349–1359, 2009. doi: 10.1109/
 328 TCSI.2008.2006649.
- 329 Song Han, Huizi Mao, and William J. Dally. Deep compression: Compressing deep neural net-
 330 work with pruning, trained quantization and huffman coding. Computer Vision and Pattern
 331 Recognition, 2015a.

- 332 Song Han, Jeff Pool, John Tran, and William Dally. Learning both weights and connections for
333 efficient neural network. In C. Cortes, N. Lawrence, D. Lee, M. Sugiyama, and R. Garnett (eds.),
334 Advances in Neural Information Processing Systems, volume 28. Curran Associates, Inc., 2015b.
- 335 Geoffrey Hinton, Oriol Vinyals, and Jeff Dean. Distilling the knowledge in a neural network, 2015.
- 336 Andrew Howard, Mark Sandler, Bo Chen, Weijun Wang, Liang-Chieh Chen, Mingxing Tan, Grace
337 Chu, Vijay Vasudevan, Yukun Zhu, Ruoming Pang, Hartwig Adam, and Quoc Le. Searching
338 for mobilenetv3. In 2019 IEEE/CVF International Conference on Computer Vision (ICCV), pp.
339 1314–1324, 2019. doi: 10.1109/ICCV.2019.00140.
- 340 Gao Huang, Yu Sun, Zhuang Liu, Daniel Sedra, and Kilian Weinberger. Deep networks with stochas-
341 tic depth, 2016.
- 342 Jonathan Krause, Michael Stark, Jia Deng, and Li Fei-Fei. 3d object representations for fine-grained
343 categorization. In 2013 IEEE International Conference on Computer Vision Workshops, pp. 554–
344 561, 2013. doi: 10.1109/ICCVW.2013.77.
- 345 Alex Krizhevsky. Learning multiple layers of features from tiny images. 2009.
- 346 Changlin Li, Tao Tang, Guangrun Wang, Jiefeng Peng, Bing Wang, Xiaodan Liang, and Xiaojun
347 Chang. Bossnas: Exploring hybrid cnn-transformers with block-wisely self-supervised neural
348 architecture search. In 2021 IEEE/CVF International Conference on Computer Vision (ICCV),
349 pp. 12261–12271, 2021. doi: 10.1109/ICCV48922.2021.01206.
- 350 Yuhang Li, Xin Dong, and Wei Wang. Additive powers-of-two quantization: An efficient
351 non-uniform discretization for neural networks. In International Conference on Learning
352 Representations, 2020.
- 353 Ji Lin, Wei-Ming Chen, Yujun Lin, John Cohn, Chuang Gan, and Song Han. Mccnet: Tiny deep
354 learning on iot devices. In H. Larochelle, M. Ranzato, R. Hadsell, M.F. Balcan, and H. Lin
355 (eds.), Advances in Neural Information Processing Systems, volume 33, pp. 11711–11722. Curran
356 Associates, Inc., 2020.
- 357 Ji Lin, Wei-Ming Chen, Han Cai, Chuang Gan, and Song Han. Memory-efficient patch-based in-
358 ference for tiny deep learning. In M. Ranzato, A. Beygelzimer, Y. Dauphin, P.S. Liang, and
359 J. Wortman Vaughan (eds.), Advances in Neural Information Processing Systems, volume 34, pp.
360 2346–2358. Curran Associates, Inc., 2021a.
- 361 Ji Lin, Ligeng Zhu, Wei-Ming Chen, Wei-Chen Wang, Chuang Gan, and Song Han. On-device
362 training under 256kb memory. In S. Koyejo, S. Mohamed, A. Agarwal, D. Belgrave, K. Cho, and
363 A. Oh (eds.), Advances in Neural Information Processing Systems, volume 35, pp. 22941–22954.
364 Curran Associates, Inc., 2022.
- 365 Yujun Lin, Mengtian Yang, and Song Han. Naas: Neural accelerator architecture search. In 2021
366 58th ACM/IEEE Design Automation Conference (DAC), pp. 1051–1056, 2021b. doi: 10.1109/
367 DAC18074.2021.9586250.
- 368 Zhouhan Lin, Matthieu Courbariaux, Roland Memisevic, and Yoshua Bengio. Neural networks with
369 few multiplications, 2016.
- 370 Chenxi Liu, Liang-Chieh Chen, Florian Schroff, Hartwig Adam, Wei Hua, Alan L. Yuille, and
371 Li Fei-Fei. Auto-deeplab: Hierarchical neural architecture search for semantic image segmenta-
372 tion. In 2019 IEEE/CVF Conference on Computer Vision and Pattern Recognition (CVPR), pp.
373 82–92, 2019a. doi: 10.1109/CVPR.2019.00017.
- 374 Hanxiao Liu, Karen Simonyan, and Yiming Yang. Darts: Differentiable architecture search. In
375 International Conference on Learning Representations, 2019b.
- 376 Huizi Mao, Song Han, Jeff Pool, Wenshuo Li, Xingyu Liu, Yu Wang, and William J. Dally. Ex-
377 ploring the granularity of sparsity in convolutional neural networks. In 2017 IEEE Conference
378 on Computer Vision and Pattern Recognition Workshops (CVPRW), pp. 1927–1934, 2017. doi:
379 10.1109/CVPRW.2017.241.

- 380 Pavlo Molchanov, Stephen Tyree, Tero Karras, Timo Aila, and Jan Kautz. Pruning convolutional neural networks for resource efficient inference. In International Conference on Learning Representations, 2017.
- 383 Maria-Elena Nilsback and Andrew Zisserman. Automated flower classification over a large number
384 of classes. In 2008 Sixth Indian Conference on Computer Vision, Graphics Image Processing,
385 pp. 722–729, 2008. doi: 10.1109/ICVGIP.2008.47.
- 386 Cristina Palmero, Abhishek Sharma, Karsten Behrendt, Kapil Krishnakumar, Oleg V. Komogortsev,
387 and Sachin S. Talathi. Openeds2020: Open eyes dataset, 2020.
- 388 Omkar M Parkhi, Andrea Vedaldi, Andrew Zisserman, and C. V. Jawahar. Cats and dogs. In
389 2012 IEEE Conference on Computer Vision and Pattern Recognition, pp. 3498–3505, 2012. doi:
390 10.1109/CVPR.2012.6248092.
- 391 Mohammad Rastegari, Vicente Ordonez, Joseph Redmon, and Ali Farhadi. Xnor-net: Imagenet
392 classification using binary convolutional neural networks, 2016.
- 393 Sebastian Ruder. An overview of multi-task learning in deep neural networks, 2017.
- 394 Mark Sandler, Andrew Howard, Menglong Zhu, Andrey Zhmoginov, and Liang-Chieh Chen. Mo-
395 bilenetv2: Inverted residuals and linear bottlenecks. In 2018 IEEE/CVF Conference on Computer
396 Vision and Pattern Recognition(CVPR), pp. 4510–4520, 2018. doi: 10.1109/CVPR.2018.00474.
- 397 Huihong Shi, Haoran You, Yang Zhao, Zhongfeng Wang, and Yingyan Lin. Nasa: Neural ar-
398 chitecture search and acceleration for hardware inspired hybrid networks. In 2022 IEEE/ACM
399 International Conference On Computer Aided Design (ICCAD), pp. 1–9, 2022.
- 400 Dehua Song, Yunhe Wang, Hanting Chen, Chang Xu, Chunjing Xu, and Dacheng Tao. Adders:
401 Towards energy efficient image super-resolution. In 2021 IEEE/CVF Conference on Computer
402 Vision and Pattern Recognition(CVPR), pp. 15643–15652, 2021. doi: 10.1109/CVPR46437.
403 2021.01539.
- 404 Nitish Srivastava, Geoffrey Hinton, Alex Krizhevsky, Ilya Sutskever, and Ruslan Salakhutdinov.
405 Dropout: A simple way to prevent neural networks from overfitting. J. Mach. Learn. Res., 15(1):
406 1929–1958, jan 2014. ISSN 1532-4435.
- 407 Statista. Internet of things (iot) connected devices installed base worldwide from 2015
408 to 2025. Website, 2016. [https://www.statista.com/statistics/471264/
409 iot-number-of-connected-devices-worldwide/](https://www.statista.com/statistics/471264/iot-number-of-connected-devices-worldwide/).
- 410 Mingxing Tan, Bo Chen, Ruoming Pang, Vijay Vasudevan, Mark Sandler, Andrew Howard, and
411 Quoc V. Le. Mnasnet: Platform-aware neural architecture search for mobile. In 2019 IEEE/CVF
412 Conference on Computer Vision and Pattern Recognition (CVPR), pp. 2815–2823, 2019. doi:
413 10.1109/CVPR.2019.00293.
- 414 Kuan Wang, Zhijian Liu, Yujun Lin, Ji Lin, and Song Han. Haq: Hardware-aware automated quan-
415 tization with mixed precision, 2019.
- 416 Yunhe Wang, Mingqiang Huang, Kai Han, Hanting Chen, Wei Zhang, Chunjing Xu, and Dacheng
417 Tao. Addernet and its minimalist hardware design for energy-efficient artificial intelligence, 2021.
- 418 Bichen Wu, Alvin Wan, Xiangyu Yue, Peter Jin, Sicheng Zhao, Noah Golmant, Amir Gholaminejad,
419 Joseph Gonzalez, and Kurt Keutzer. Shift: A zero flop, zero parameter alternative to spatial con-
420 volutions. In 2018 IEEE/CVF Conference on Computer Vision and Pattern Recognition(CVPR),
421 pp. 9127–9135, 2018. doi: 10.1109/CVPR.2018.00951.
- 422 Bichen Wu, Xiaoliang Dai, Peizhao Zhang, Yanghan Wang, Fei Sun, Yiming Wu, Yuandong Tian,
423 Peter Vajda, Yangqing Jia, and Kurt Keutzer. Fbnet: Hardware-aware efficient convnet design via
424 differentiable neural architecture search. In 2019 IEEE/CVF Conference on Computer Vision and
425 Pattern Recognition (CVPR), pp. 10726–10734, 2019. doi: 10.1109/CVPR.2019.01099.

- 426 Ping Xue and Bede Liu. Adaptive equalizer using finite-bit power-of-two quantizer. IEEE
 427 Transactions on Acoustics, Speech, and Signal Processing, 34(6):1603–1611, 1986. doi:
 428 10.1109/TASSP.1986.1164999.
- 429 Haoran You, Xiaohan Chen, Yongan Zhang, Chaojian Li, Sicheng Li, Zihao Liu, Zhangyang Wang,
 430 and Yingyan Lin. Shiftaddnet: A hardware-inspired deep network. In H. Larochelle, M. Ranzato,
 431 R. Hadsell, M.F. Balcan, and H. Lin (eds.), Advances in Neural Information Processing Systems,
 432 volume 33, pp. 2771–2783. Curran Associates, Inc., 2020.
- 433 Haoran You, Baopu Li, Huihong Shi, Yonggan Fu, and Yingyan Lin. Shiftaddnas: Hardware-
 434 inspired search for more accurate and efficient neural networks, 2022.
- 435 Haoran You, Huihong Shi, Yipin Guo, Yingyan, and Lin. Shiftaddvit: Mixture of multiplication
 436 primitives towards efficient vision transformer, 2023.
- 437 Jiahui Yu, Pengchong Jin, Hanxiao Liu, Gabriel Bender, Pieter-Jan Kindermans, Mingxing Tan,
 438 Thomas Huang, Xiaodan Song, Ruoming Pang, and Quoc Le. Bignas: Scaling up neural archi-
 439 tecture search with big single-stage models. In European Conference on Computer Vision,
 440 2020.
- 441 Yang Zhao, Chaojian Li, Yue Wang, Pengfei Xu, Yongan Zhang, and Yingyan Lin. Dnn-chip predic-
 442 tor: An analytical performance predictor for dnn accelerators with various dataflows and hardware
 443 architectures. In ICASSP 2020 - 2020 IEEE International Conference on Acoustics, Speech and
 444 Signal Processing (ICASSP), pp. 1593–1597, 2020. doi: 10.1109/ICASSP40776.2020.9053977.

445 A ABLATION STUDY OF TRAINING SETTINGS

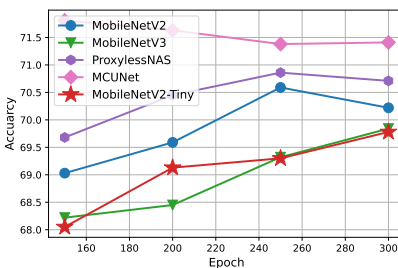


Figure 6: Baseline accuracy with training epochs.

- 446 More training epochs can improve accuracy as shown in Fig. 6. However, training for too long may
 447 produce overfitting on the augmented model and require more training time. As a trade-off, we
 448 choose to train 250 epochs on the datasets such as CIFAR-10/100. A similar ablation study on
 449 ImageNet can be found in NetAug(Cai et al., 2022).

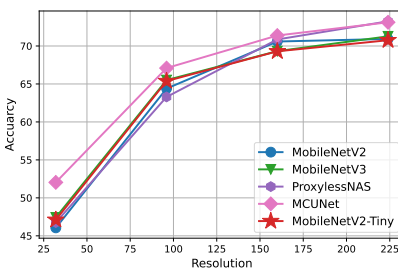


Figure 7: Baseline accuracy with different input resolution.

- 450 As shown in Fig. 6, higher resolution improves the accuracy but introduces more computation.
 451 We decided that all inputs should be resized to 160 during training and inference. Our model has
 452 a smaller capacity, allowing it to consume less energy than previous work with larger resolutions.
 453 This setting also means our experimental conclusions won't be limited to low-resolution datasets.

454 B THE SPECIFIC MEANING OF METHOD

- 455 • Base: directly trained multiplicative model.
- 456 • NetAug: multiplicative model with multiplicative augmentation.
- 457 • Shift: directly trained shift-model with ShiftConv in DeepShift(Elhoushi et al., 2021).
- 458 • AugShift: ShiftConv with multiplicative augmentation.
- 459 • Add: directly trained add-model with AddConv in AdderNet(Chen et al., 2020).
- 460 • AugAdd: AddConv with multiplicative augmentation.
- 461 • ShiftAddAug (Mult-free): results of neural architecture search with shift/add operator only
- 462 • ShiftAddAug: results of neural architecture search with shift/add/multi. operator

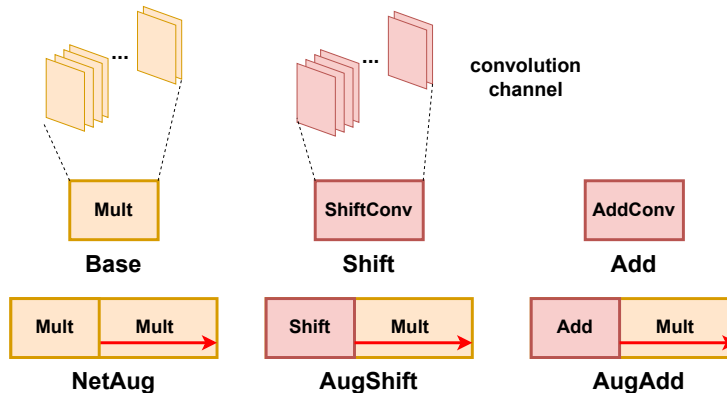


Figure 8: Schematic diagram of each method.

463 C MORE ABLATION STUDY OF HETEROGENEOUS WEIGHT SHARING

464 **The difference from ShiftAddNas.** When we encountered the issue of weight tearing, we first
 465 thought of the solution in ShiftAddNAS(You et al., 2022). However, when we applied it, the train-
 466 ing loss didn't converge, which made us believe that the method was not suitable for our training
 467 situation and it was difficult to compare performance. ShiftAddNas sorts the values of weights,
 468 dividing them into n groups from bottom to top, and then sets n learnable parameters to scale the
 469 weight values within each group. Our HWS strategy uses fully connected to remap the Conv ker-
 470 nel and use Equ.5 to handle different weight distributions. The obtained result is only added to the
 471 original weight as a bias, rather than applied directly. We use directly trained multiplicative and
 472 multiplication-free Conv weights as datasets to train the FC layer here, and freeze it in augmented
 473 training. We believe that our method has better training stability than ShiftAddNas. As shown in
 474 Tab.8, the ShiftAddNas method and direct mapping with learnable Linear will make it unable to
 475 train.

Table 8: The ablation study of different method for HWS

Method	MobileNetV2 w0.35	MobileNetV3 w0.35	MCUNet	ProxylessNAS w0.35	MobileNet-tiny
ShiftAddNAS	Nan	Nan	Nan	Nan	Nan
Linear remap	Nan	Nan	Nan	Nan	Nan
KL-loss only	69.84	69.98	71.12	70.52	68.70
Linear + skip connect + freeze	71.02	72.70	74.44	72.99	71.08
Ours	71.83	73.37	74.59	73.86	71.89

476 **Is HWS a parameterization trick that can directly improve the target model?** We designed this
 477 ablation study to demonstrate that our HWS remapping method does not improve the accuracy of
 478 multiplication-free NNs by itself. On the contrary, it slightly damages the accuracy of the model.
 479 This kind of remapping is only a compensation method for different weight distributions, and will
 480 not produce gain for directly trained multiplication-free NNs.

Table 9: HWS is not a parameterization trick that can directly improve target model

Method	MobileNetV2 w0.35	MobileNetV3 w0.35	MCUNet	ProxylessNAS w0.35	MobileNet-tiny
w/o. augmentation, w/o. HWS	69.25	68.42	70.87	70.54	68.29
w/o. augmentation, with HWS	68.32	68.10	71.13	69.88	68.02
with augmentation, with HWS	71.83	73.37	74.59	73.86	71.89

481 D SHIFTADDAUG IN SPECIFIC TASKS FOR IOT DEVICES

482 To demonstrate the effectiveness of our method in specific applications, we apply ShiftAddAug to a
 483 semantic segmentation task for IoT devices.

484 The segmentation of iris, pupil and sclera plays an important role in eye tracking in VR devices.
 485 To cope with this task, it is highly cost-effective to use fast and energy-efficient multiplication-free
 486 neural networks on such devices. OpenEDS(Palmero et al., 2020) is a large scale dataset of eye-
 487 images captured using a virtual-reality (VR) devices. We train each model from scratch for 100
 488 epochs with a learning rate of 0.001 and batch size of 8. The mIoU(%) of the segmentation results
 489 of each model are shown in Tab.10 .

Table 10: ShiftAddAug on OpenEDS dataset for semantic segmentation task

Method	MobileNetV2 w0.35	ProxylessNAS w0.35
Base/NetAug	88.68 / 92.41	86.27 / 92.84
Shift/AugShift	88.01 / 94.52	86.01 / 95.12
Add/AugAdd	83.94 / 91.20	82.01 / 90.45

490 From the results shown in Fig.9, we can see that the model trained with augmentation will have
 491 fewer abnormal segmentation areas.

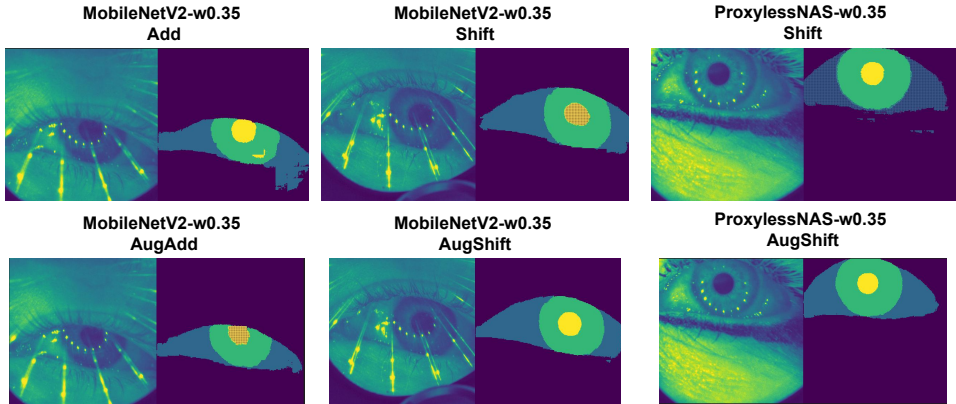


Figure 9: ShiftAddAug on OpenEDS.

492 E MORE TRAINING DETAILS

493 For ImageNet, we train models with batch size 768 on 6 GPUs. We use the SGD optimizer with
 494 Nesterov momentum of 0.9 and weight decay 4e-5. The initial learning rate is 0.15 and gradually
 495 decreases to 0 following the cosine schedule. Label smoothing is used with a factor of 0.1. We train
 496 150 epochs with the multiplicative model and then finetune 100 epochs for the Shift model with the
 497 same setting. The models with AddConv are trained from scratch for 300 epochs.

498 For CIFAR10, we use pre-trained weights from CIFAR100 with original Conv and finetune 100
 499 epochs for the Shift model. The models with AddConv are trained from scratch for 300 epochs on
 500 2 GPUs. For other datasets, we load pre-trained weights from ImageNet and finetune with the same
 501 settings.

502 For the neural architecture search, we changed the model structures based on MCUNet and Mo-
 503 bileNetV3 and pre-explored 100 model structures that met the hardware requirements. Energy con-
 504 sumption and latency can be easily obtained. We start training from the model that meets the condi-
 505 tions with the largest computational amount. Evolutionary algorithms are then used to explore other
 506 model structures. Any setting that exceeds the hardware limit will be stopped early and output 0%
 507 accuracy as a penalty. We trained them for 30 epochs for quick exploration and trained the top 10
 508 for the full 300-epoch training.

509 For ShiftConv, its weights are quantized to 5 bits, and activations are quantized to 16 bits during
 510 calculation. For AddConv, all calculations are performed under 32bit.

511 For HWS, we take the weights on the convolution kernel as input into the FC. The FC has a hidden
 512 layer enlarged by a factor of 8. Then values goes through distribution remapping to get the output.
 513 This section is pre-trained using independently trained model weights. We assume that this mapping
 514 is generalizable and freezes its weights when training the final model.

515 F COMPARED WITH MULTIPLICATION-FREE NNs

Method	Backbone	Resolution	Params(M)	Mult(M)	Shift(M)	Add(M)	CIFAR100 Accy(%)	Energy(mj)	Latency(ms)
DeepShift/ AugShift	MobileNetV2-w0.35	160	0.52	0	29.72	29.72	69.25 / 71.83	0.74	0.246
	MobileNetV2-w1.0	32	2.4	0	94.72	94.72	72.39	1.749	0.821
	MobileNetV2-Tiny	160	0.35	0	27.31	27.31	68.29 / 71.89	0.697	0.228
	MobileNetV3-w0.35	160	0.96	0	18.35	18.35	68.42 / 73.37	0.536	0.16
	MCUNet	160	0.59	0	65.72	65.72	70.87 / 74.59	1.323	0.545
	ProxylessNAS-w0.35	160	0.63	0	34.56	34.56	70.54 / 73.86	0.774	0.294
	ResNet-18	32	11.05	0	549.18	549.18	73.92	8.39	7.158
VGG19	32	20.08	0	399.21	399.21	62.68	7.603	5.192	
AdderNet/ AugAdd	MobileNetV2-w0.35	160	0.52	4.52	0	56.88	67.85 / 69.38	1.091	0.753
	MobileNetV2-Tiny	160	0.35	4.43	0	52.09	66.57 / 67.65	0.999	0.693
	MCUNet	160	0.59	20.91	0	113.09	70.25 / 72.72	2.345	1.72
	ProxylessNAS-w0.35	160	0.63	8.81	0	61.97	68.87 / 70.18	1.281	0.881
	ResNet-20	32	0.28	0.56	0	102.7	67.6	1.802	1.434
	ResNet-32	32	0.47	0.56	0	174.6	69.02	3.038	2.428
VGG-small	32	20.3	0	0	920	72.73	16	15.11	
ShiftAddNet	ResNet-20	32	1.13	0	40.8	127.17	58.5	2.07	2.315
	VGG19	32	83.52	0	398	1380	65	24.68	25.632
ShiftAddNAS	mult-free	32	-	3	35	48	71.0	-	-
	hybrid	32	-	22	21	62	78.6	-	-
ShiftAddAug	mult-free (NAS)	160	1.3	0.13	33.5	33.6	74.61	0.851	0.264
	hybrid (NAS)	96	2.3	16.2	20.2	36.4	78.72	2.431	0.644